Supporting Information for: Highly tunable layered exciton in bilayer WS_2: linear quantum confined Stark effect versus electrostatic doping

Sarthak Das,[†] Medha Dandu,[†] Garima Gupta,[†] Krishna Murali,[†] Nithin Abraham,[†] Sangeeth Kallatt,[‡] Kenji Watanabe,[¶] Takashi Taniguchi,[§] and Kausik Majumdar[*,†]

†*Department of Electrical Communication Engineering, Indian Institute of Science, Bangalore 560012, India*

‡*Center for Quantum Devices, Niels Bohr Institute, University of Copenhagen, Denmark*

¶*Research Center for Functional Materials, National Institute for Materials Science, 1-1 Namiki, Tsukuba 305-044, Japan*

§*International Center for Materials Nanoarchitectonics, National Institute for Materials Science, 1-1 Namiki, Tsukuba, 305-044 Japan*

E-mail: kausikm@iisc.ac.in

S1. Stark shift calculation of the excitons in bilayer TMD:

The bilayer Hamiltonian (H) with an inter-layer potential difference of $2U$ for WS_2 can be written as[1,2]

$$H = \begin{bmatrix} \Delta - U & at_i(\nu_z k_x + ik_y) & 0 & 0 \\ at_i(\nu_z k_x - ik_y) & -\nu_z s_z \lambda - U & 0 & t_\perp \\ 0 & 0 & \Delta + U & at_i(\nu_z k_x - ik_y) \\ 0 & t_\perp & at_i(\nu_z k_x + ik_y) & \nu_z s_z \lambda + U \end{bmatrix} \tag{1}$$

where Δ is the bandgap, a is the lattice constant, t_i is the nearest-neighbour intralayer hopping, λ is the spin-valley coupling for holes in monolayer, $t_\perp$ is the interlayer hopping for holes, ν_z is the valley degree of freedom, and s_z is spin degree of freedom (± 1). Material parameters are obtained from ref.[1]

An exciton state ($|\Psi\rangle_{\vec{Q}}$) in an exciton band n with center of mass momentum $\vec{Q}$ in reciprocal space can be written as[3]

$$|\Psi\rangle_{\vec{Q}} = \sum_{v,c,\vec{k}} A^n_{v,c,\vec{Q}}(\vec{k}) \left|v, \vec{k}\right\rangle \left|c, \vec{k} + \vec{Q}\right\rangle \tag{2}$$

$A^n_{v,c,\vec{Q}}(\vec{k})$ can be obtained from the solution of the Bethe-Salpeter (BS) equation[3]

$$\left\langle v, c, \vec{k}, \vec{Q} \right| H \left| v', c', \vec{k'}, \vec{Q} \right\rangle = \delta_{vv'} \delta_{cc'} \delta_{\vec{k}\vec{k'}} (\varepsilon_{(\vec{k}+\vec{Q})c} - \varepsilon_{\vec{k}v}) - (\Xi - \Lambda)^{cc'}_{vv'}(\vec{k}, \vec{k'}, \vec{Q}), \tag{3}$$

Here ε is the eigenvalue obtained by diagonalizing the quasiparticle Hamiltonian described above. Ξ and Λ are the direct and exchange term in the two-particle matrix elements. We take $\Lambda = 0$ for excitons with $Q = 0$.

To obtain the Stark effect, the above equation is solved for different U, and the corresponding exciton energy eigenvalues at $Q = 0$ are calculated. The corresponding vertical field (ξ) is calculated as

$$\xi = 2U/t_0, \tag{4}$$

where t_0 is the physical separation between two Tungsten layers ($6.3\mathring{A}$).

S2. Raman characterization of bilayer WS_2

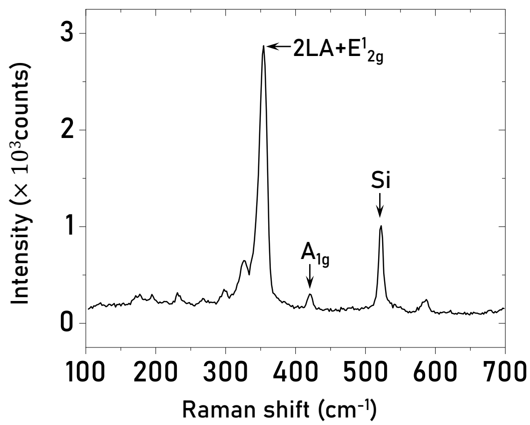

Figure S1: **Raman characterization of bilayer WS_2.** Room temperature Raman spectra for bilayer WS_2 (S1). Different Raman modes are marked in the figure.

S3. Calculation of reflectance with transfer matrix method:

The reflectance of the stacks is obtained by calculating the reflection from multiple layer dielectric formalism. For an N layer system the incident electric field ($\mathcal{E}$) can be written as[4]

$$\begin{bmatrix} \mathcal{E}_1^+ \\ \mathcal{E}_1^- \end{bmatrix} = \mathcal{R} \begin{bmatrix} \mathcal{E}_{(N+2)}^+ \\ \mathcal{E}_{(N+2)}^- \end{bmatrix} \tag{5}$$

where $\mathcal{E}_j^+$, $\mathcal{E}_j^-$ are the incoming and outgoing electric field from the j^{th} surface

$$\mathcal{R} = \mathcal{R}_1\mathcal{R}_2...\mathcal{R}_{N+1} \tag{6}$$

and, under normal incidence,

$$\mathcal{R}_j = \frac{1}{\tau_j} \begin{bmatrix} \exp(i\delta_j) & \rho_j \exp(i\delta_j) \\ \rho_j \exp(-i\delta_j) & \exp(-i\delta_j) \end{bmatrix} \tag{7}$$

$$\delta_1 = 0, \delta_j = k_j t_j = (2\pi/\lambda)\tilde{n}_j t_j \tag{8}$$

$$\tau_j = \frac{2\tilde{n}_j}{\tilde{n}_j + \tilde{n}_{j+1}}, \rho_j = \frac{\tilde{n}_j - \tilde{n}_{j+1}}{\tilde{n}_j + \tilde{n}_{j+1}} \tag{9}$$

Here τ is the transmission coefficient, ρ is the reflection coeffecient and $\tilde{n}$ is the complex refractive index of the individual layers with thickness t. Further $\tilde{n}$ defined as $\tilde{n}$=n-iκ with κ is the extinction coefficient of the material.

The reflection from the stack is defined by $R = \left|\mathcal{E}_1^-/\mathcal{E}_1^+\right|^2$, which is calculated for the stacks with (R_{on}) and without (R_{off}) the bilayer WS_2 layer. Complex refractive index ($\tilde{n}$) of graphite, Si and SiO_2 with wavelength dispersion are taken from literature,[5,6] κ of hBN is assumed to be zero with n of 1.85.[7] The $\tilde{n}$ value for WS_2 is obtained from the Lorentzian oscillator model described in the main text. To fit the differential reflectance spectra ($\frac{\Delta R}{R}$) obtained from the experiment, we further calculate $\frac{\Delta R}{R} = \frac{R_{on}-R_{off}}{R_{off}}$.

S4. Gate leakage current

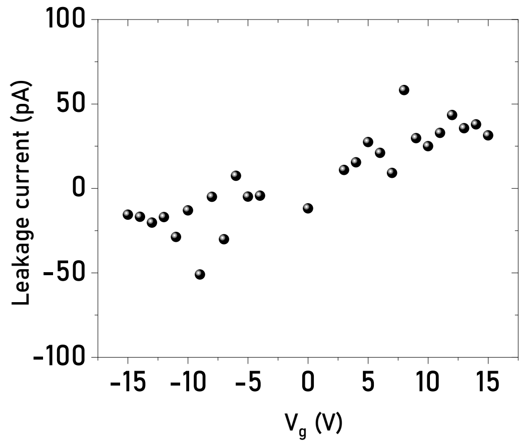

Figure S2: **Gate leakage current for sample S2.** Measured gate leakage current for the experimental range of applied gate voltage for the sample S2.

S5. Field dependent reflectance spectra for device configuration S2-F

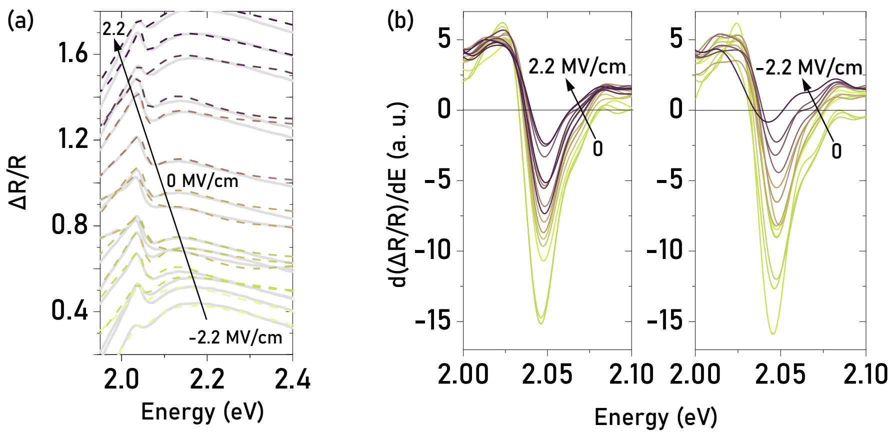

Figure S3: **Field dependent reflectance spectra for device configuration S2-F.** (a) Field dependent differential reflectance for the device configuration S2-F. (b) First derivative of the differential reflectance of bilayer WS_2 with the applied vertical field (in $MVcm^{-1}$), measured at 4.2 K. The left and the right panels show the positive and negative electric field, respectively.

S6. Temperature dependent reflectance spectra for sample S3

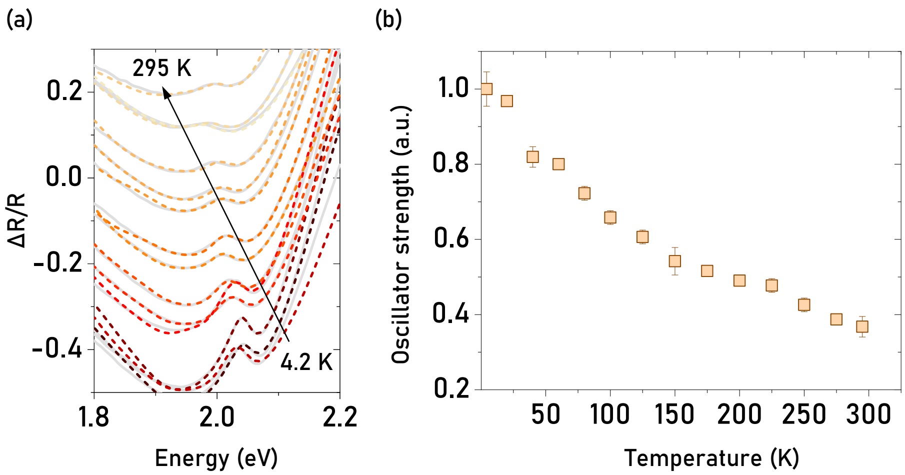

Figure S4: **Temperature dependent reflectance spectra for sample S3.** (a) Temperature dependent differential reflectance for the sample S3. Here the bilayer WS_2 is directly sitting on few layer graphene enhancing the fast nonradiative processes. (b) Normalized oscillator strength of the exciton extracted from the fitting across the temperature range.

S7. Gate dependent reflectance spectra for device configuration S2-D

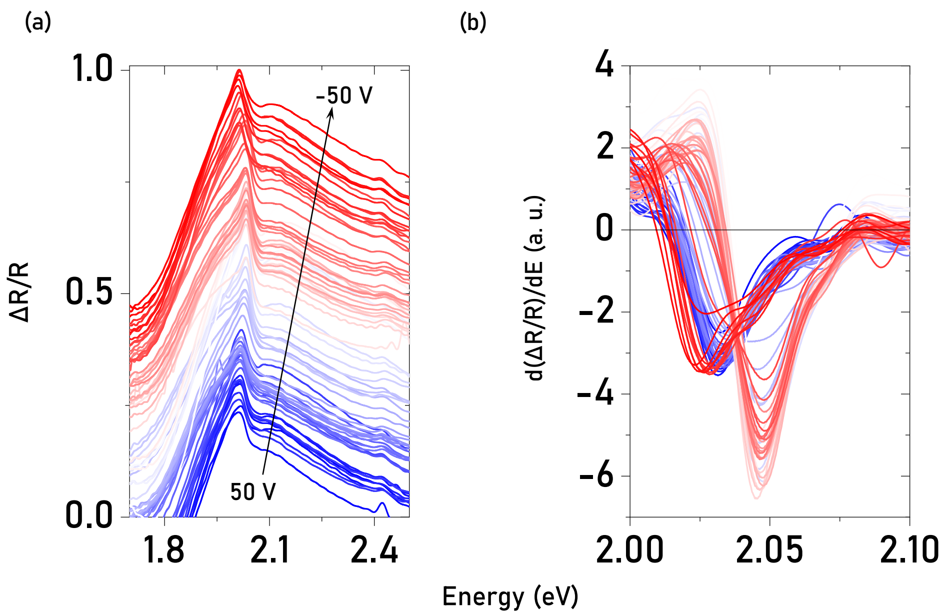

Figure S5: **Gate dependent reflectance spectra for device configuration S2-D.** (a) Gate dependent differential reflectance spectra for the device configuration S2-D showing the electrostatic doping and the transfer of oscillator strength from exciton to trion at higher gate voltage. (b) First derivative of the reflectance spectra in the same voltage range.

S8. Optical images of the stacks

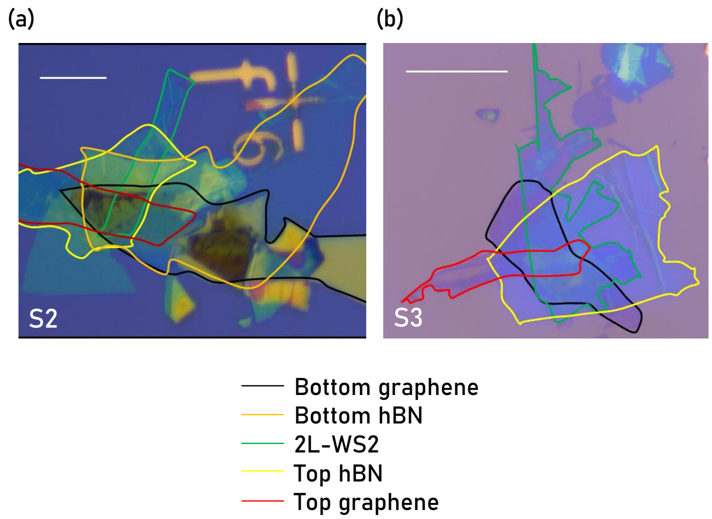

Figure S6: **Optical images of the stacks in sample S2 and S3.** (a-b) Optical image of the complete stacks of sample S2 and S3. The different layer boundaries are marked with different colors. The scale bar is 20 μm.

References

(1) Gong, Z.; Liu, G.-B.; Yu, H.; Xiao, D.; Cui, X.; Xu, X.; Yao, W. Magnetoelectric effects and valley-controlled spin quantum gates in transition metal dichalcogenide bilayers. *Nature communications* **2013**, *4*, 1–6.

(2) Das, S.; Gupta, G.; Majumdar, K. Layer degree of freedom for excitons in transition metal dichalcogenides. *Physical Review B* **2019**, *99*, 165411.

(3) Wu, F.; Qu, F.; Macdonald, A. H. Exciton band structure of monolayer MoS 2. *Physical Review B* **2015**, *91*, 075310.

(4) Ghatak, A. K.; Thyagarajan, K.; Tiyākarāca_n, K. *Optical electronics*; Cambridge University Press, 1989.

(5) Djurišić, A. B.; Li, E. H. Optical properties of graphite. *Journal of applied physics* **1999**, *85*, 7404–7410.

(6) Palik, E. D. *Handbook of optical constants of solids*; Academic press, 1998; Vol. 3.

(7) Golla, D.; Chattrakun, K.; Watanabe, K.; Taniguchi, T.; LeRoy, B. J.; Sandhu, A. Optical thickness determination of hexagonal boron nitride flakes. *Applied Physics Letters* **2013**, *102*, 161906.